Classical ferromagnet with double-exchange interaction: High-resolution Monte Carlo simulations

A. A. Caparica
Instituto de Física, Universidade Federal de Goiás, Caixa Postal 131, Goiânia GO, CEP 74001-970, Brazil
and Center for Simulational Physics, The University of Georgia, Athens, Georgia 30602

Alex Bunker and D. P. Landau
Center for Simulational Physics, The University of Georgia, Athens, Georgia 30602
(Received 30 June 1999)

A high-resolution Monte Carlo study has been carried out for a classical ferromagnet on the simple cubic lattice with double-exchange interaction. The static critical exponents were determined as $\nu=0.6949(38)$, $\beta=0.3535(30)$, and $\gamma=1.3909(30)$. Comparison of these values, as well as the value of the fourth-order cumulant at the transition temperature, with those for the classical Heisenberg model leads to the conclusion that these systems belong to the same universality class. Some comparisons with experiment are presented.

I. INTRODUCTION

The recent discovery of anomalously large magnetoresistance effects near the Curie temperature in doped rare-earth perovskite manganites, $A_{1-x}B_x\mathrm{MnO_3}$ ($A=$La,Pr,Nd and $B=$Ca, Ba,Sr,Pb) has led to an increasing interest in these materials because of both the new physics involved and of the possible technological applications. Traditionally the properties of the perovskite manganites have been explained by double-exchange theory.[1] The basic idea of double exchange is that each Mn ion has a core spin of $S_c=3/2$, and a fraction $(1-x)$ have an extra electron in the E_g orbitals with spin parallel to the core spin due to strong intrasite exchange. When an electron hops from site i to site j its spin must also change from being parallel to $\mathbf{S}_c^i$ to being parallel to $\mathbf{S}_c^j$, but with an energy loss proportional to the cosine of half the angle between the core spins.[2] Although the double-exchange mechanism provides a good qualitative explanation for the ''colossal'' magnetoresistance (CMR), it has been suggested by several authors that it cannot alone describe this phenomenon. They propose that, in addition to the double exchange, a complete understanding of these materials should include strong electron correlations,[3] a strong electron-phonon interaction,[4] or coexisting phases.[7] Nevertheless, there are also attempts to describe CMR behavior exclusively in the framework of the double-exchange mechanism.[5,6] Such a scenario suggests that a high-precision study of the classical ferromagnet with double-exchange interaction would be an important reference point for the evaluation of the real role of the double-exchange in the CMR materials. Monte Carlo computer simulations currently are a powerful tool to investigate critical phenomena, and we present here results of a high-resolution Monte Carlo study of the static critical behavior of the simple cubic classical ferromagnet with double-exchange interaction. The analysis of the data is carried out by combining finite-size scaling[10–12] and cumulant methods;[13–18] applying the reweighting technique[8,9] we obtain the fourth-order cumulants and determine the location and value of the extrema of various thermodynamic quantities. The model is defined and simulational techniques and data analysis are described in some detail in Sec. II. Results are presented in Sec. III and we summarize and conclude in Sec. IV.

II. BACKGROUND

A. Model

We are interested in a classical spin model for an isotropic ferromagnet on the simple cubic lattice with double-exchange interaction. The Hamiltonian for such system is given by[2]

$$\mathcal{H}=-\sum_{\langle i,j\rangle} J\sqrt{1+\mathbf{S}_i\cdot\mathbf{S}_j}, \tag{1}$$

where J is the ferromagnetic coupling constant and the spin $\mathbf{S}_i=(S_i^x,S_j^y,S_k^z)$ is of O(3) symmetry and unit length in the spin space. We consider $L\times L\times L$ systems with nearest-neighbor interactions and periodic boundary conditions, so that the sum in Eq. (1) runs over all nearest-neighbor pairs of lattice sites. The basic thermodynamic quantities of interest are the total energy E and the magnetization m. In discussing the critical properties of this model we will work with the dimensionless coupling constant K related to the interaction constant J by $K=J/k_BT$, where k_B is the Boltzman's constant and T is the absolute temperature.

B. Simulations

We have simulated $L\times L\times L$ simple cubic lattices with periodic boundary conditions and dimensions $L=10$, 14, 20, 30, and 40. Sampling was performed using the single spin flip Metropolis[20] Monte Carlo technique. We used a checkerboard algorithm, and one Monte Carlo (MC) step is defined as the attempt to flip every spin in the lattice once. For each simulation, 1000 steps were initially discarded and then 10^6 MC steps were considered for each run. The number of runs varied according to the behavior of the error bars for different thermodynamic functions and also the size of the

lattice. The greater the lattice size the greater the number of runs required to reach the desired precision. Because of these limitations the $L=40$ lattice was taken into account only in some of our calculations. A minimal number of 6 runs was taken for the $10\times10\times10$ lattice, while the $30\times30\times30$ lattice demanded up to 28 runs in some cases.

C. Finite-size scaling and the histogram method

According to finite-size scaling theory[10–12] the singular part of the reduced free energy can be described phenomenologically by an universal scaling form

$$f(t,H;L)=L^{-d}Y(atL^{1/\nu},bHL^{\Delta/\nu}), \tag{2}$$

where $t=(T_c-T)/T_c$ is the reduced temperature, H is the external ordering field, a and b are metric factors making the scaling function Y universal, d is the spatial dimension of the system (equal to 3 in our case), and ν and Δ are static critical exponents. From the definition of the free energy one can obtain scaling forms for several thermodynamic quantities, such as the zero field expressions for the magnetization, susceptibility, and specific heat, respectively,

$$m\approx L^{-\beta/\nu}\mathcal{M}(tL^{1/\nu}), \tag{3}$$

$$\chi\approx L^{\gamma/\nu}\mathcal{X}(tL^{1/\nu}), \tag{4}$$

$$c\approx c_\infty+L^{\alpha/\nu}\mathcal{C}(tL^{1/\nu}), \tag{5}$$

where α, β, and γ are also static critical exponents which should satisfy the scaling and hyperscaling relations[19]

$$\Delta=\beta\delta=\beta+\gamma, \tag{6}$$

$$2-\alpha=d\nu=2\beta+\gamma. \tag{7}$$

Estimates for the critical temperature can be carried out by the ''cumulant crossing'' method introduced by Binder and Stauffer,[13] which scales the positions of the crossings of the fourth-order magnetization cumulant

$$U_L=1-\frac{\langle m^4\rangle_L}{3\langle m^2\rangle_L^2} \tag{8}$$

for different lattice sizes. This method does not yield very precise results, but it is important in the beginning of the simulations to locate the best values of inverse temperature where one should simulate the system. Following Ref. 21 we can define a set of thermodynamic quantities related to logarithmic derivatives of the magnetization:

$$V_1\equiv4[m^3]-3[m^4], \tag{9}$$

$$V_2\equiv2[m^2]-[m^4], \tag{10}$$

$$V_3\equiv3[m^2]-2[m^3], \tag{11}$$

$$V_4\equiv(4[m]-[m^4])/3, \tag{12}$$

$$V_5\equiv(3[m]-3[m^3])/2, \tag{13}$$

$$V_6\equiv2[m]-[m^2], \tag{14}$$

where

$$[m^n]\equiv\ln\frac{\partial\langle m^n\rangle}{\partial T}. \tag{15}$$

This set of thermodynamic quantities allows us to determine the static critical exponent ν, even though we do not yet have an estimate for the critical temperature, since using Eq. (3) it is easy to show that

$$V_j\approx(1/\nu)\ln L+\mathcal{V}_j(tL^{1/\nu}) \tag{16}$$

for $j=1,2,\ldots,6$. At the critical temperature T_c ($t=0$) the $\mathcal{V}_j$ are constants independent of the system size L. Since we have an estimate for the critical exponent ν it is possible to determine the critical temperature by locating maxima in the following quantities:[21]

$$\chi=L^3\langle(m-\langle m\rangle)^2\rangle/T, \tag{17}$$

$$D_{K_2}=\frac{\partial\langle(m-\langle m\rangle)^2\rangle}{\partial T}, \tag{18}$$

$$D_{K_3}=\frac{\partial\langle(m-\langle m\rangle)^3\rangle}{\partial T}, \tag{19}$$

$$D_{K_4}=\frac{\partial(\langle(m-\langle m\rangle)^4\rangle-\langle(m-\langle m\rangle)^2\rangle^2)}{\partial T}, \tag{20}$$

$$U_4=\frac{3\langle(m-\langle m\rangle)^2\rangle^2-\langle(m-\langle m\rangle)^4\rangle}{3\langle m\rangle^2}. \tag{21}$$

According to Eqs. (3) and (4) locations of the extrema of these functions vary asymptotically as

$$K_c(L)\approx K_c+a_qL^{-1/\nu}, \tag{22}$$

where a_q is a quantity-dependent constant, allowing then the determination of K_c. Equations (3) and (5) along with the hyperscaling relations provide the necessary tools to estimate the remaining critical static coeficients. For an accurate determination of K_c and the critical exponents we need, however, to have all these quantities as continuous functions of temperature. In order to obtain this we apply the single histogram method.[8,9] In this approach, the data contained in a histogram of the energy and the magnetization from a simulation performed at a particular value of the inverse temperature K_0 are combined to yield an optimized estimate for the density of states $W(E,M)$. The equilibrium probability distribution $P(E,M)$ for some value of K can be written as[8,9,22,23,21]

$$P_K(E,M)=\frac{H_1(E,M)e^{-\Delta KE}}{\Sigma_{E,M}H_1(E,M)e^{-\Delta KE}}, \tag{23}$$

with $\Delta K=(K-K_0)$ and where $H_1(E,M)$ is a histogram kept during the simulation, which provides an estimate for the equilibrium probability, becoming exact in the limit of an infinite-length run. In our simulation we have continuous degrees of freedom; thus the energy and the magnetization of the sampled results are from a continuum of values. For a finite-size simulation one can build up a histogram by ''binning'' the values of energy and magnetization. We can therefore evaluate the first, second, and fourth moments of the

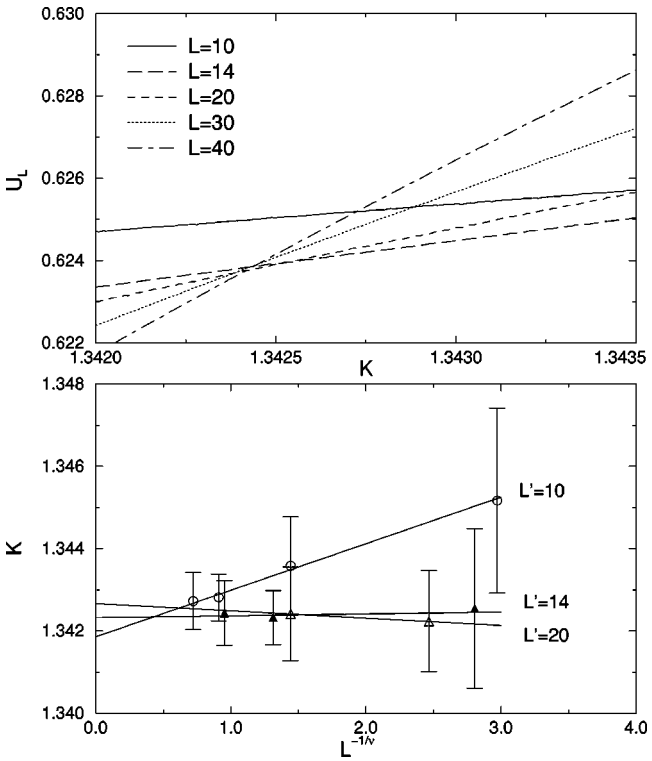

FIG. 1. (top) Variation of the fourth-order cumulant with coupling; (bottom) finite-size extrapolation of the cumulant crossings for lattices of size L and L'.

magnetization distribution, thus allowing us to determine the susceptibility, fourth-order cumulant, and all the thermodynamic functions that we presented above. Although the histogram method allows one to take derivatives and calculate the functions for temperatures other than that at which the system was simulated, one should be careful to avoid unphysical predictions of average quantities arising from inadequate accuracy in determining the ''wings'' of the distribution.

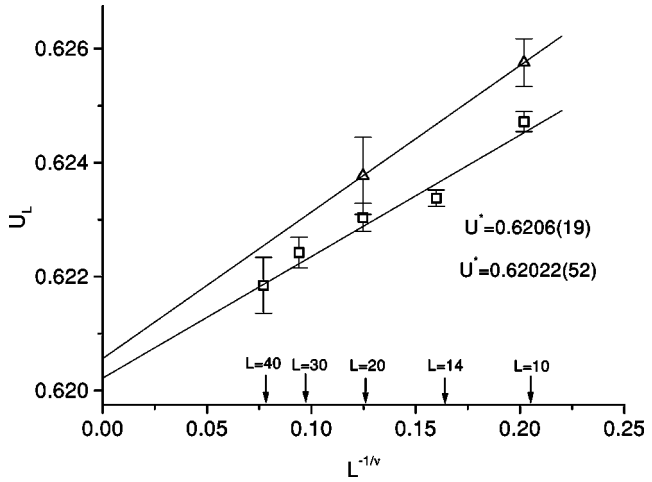

FIG. 2. Finite-size dependence of the maxima of the fourth-order cumulant: □, values at K_c; △ values at the cumulant crossings.

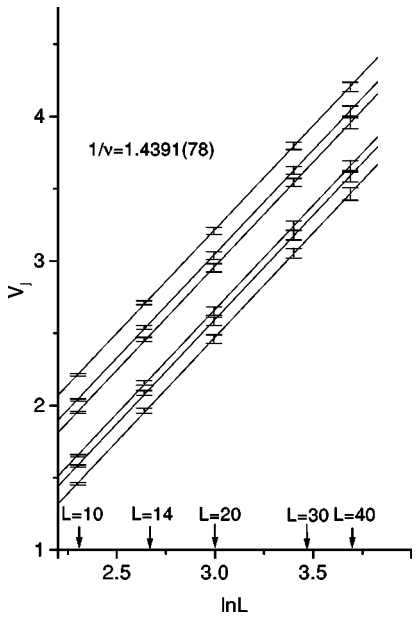

FIG. 3. Size dependence of the maxima of V_j. The slopes yield $1/\nu$.

III. RESULTS

A. Finite-size behavior of the fourth-order cumulant

A preliminary way of determining the critical temperature is to calculate the variation of the fourth-order cumulant U_L with K for various systems sizes and then locate the intersection of these curves. The values of U for two different lattice sizes L and $L'=bL$ are compared and K_c estimated by extrapolating the results of this method for $(lnb)^{-1}\rightarrow\infty$.[13] The top portion of Fig. 1 shows the pattern of fourth-order cumulant crossings and the linear fits that yield estimates for K_c in the lower portion of the figure. Not surprisingly, due to finite-size effects the fit for $L=10$ provides the less reliable result. As pointed out before this method of determining the critical temperature is not expected to be very precise; nevertheless the results are consistent with the more accurate ones that we describe below.

The value of the magnetization cumulant at the critical temperature, U^*, is an important universal quantity. We cal-

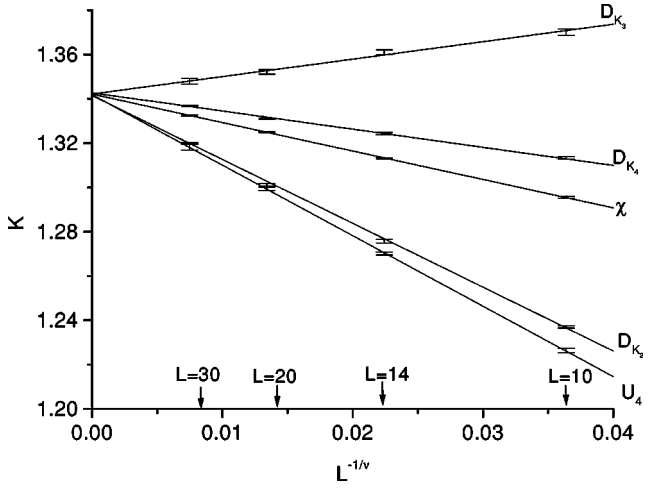

FIG. 4. Size dependence of the locations of the extrema in different thermodynamic quantities with $\nu=0.6949$.

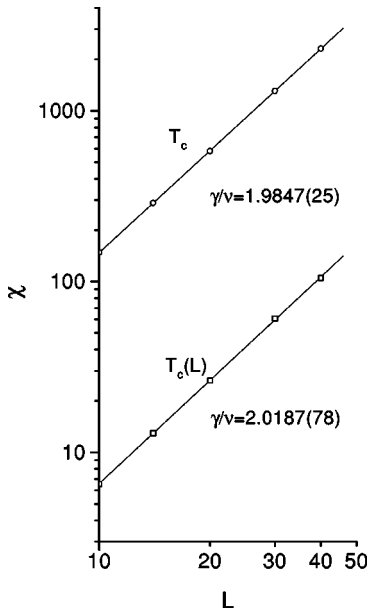

FIG. 5. Log-log plot of size dependence of (top) the finite-lattice susceptibility at $T_c(L)$; the true susceptibility at $T_c = 0.745\,15 J/k_B$. The error bars are smaller than the symbols.

culated U^* in two different ways, by determining the value of U at our estimate for K_c and by considering the values of U at the crossings for $b=2$. In Fig. 2 we show these attempts plotted versus $L^{-1/\nu}$. For the estimate from the values of U at $K=K_c$ we obtained $U^*=0.620\,22(52)$ and by cumulant crossings $U^*=0.620\,6(19)$. (The error in the estimate of U^* at $K=K_c$ is due primarily to the statistical error in the data and not the uncertainty in the location of the critical point.) This second result is consistent with the first one, but it is less precise because there are only two crossings for $b=2$; $L=10$, $L'=20$ and $L=20$, $L'=40$.

B. Determination of K_c and critical exponents from thermodynamic functions

By locating the extrema of the thermodynamic functions defined in Eqs. (9)–(14) we can determine the critical exponent ν as the inverse of the slopes of the straight lines given by Eq. (16), since at $K_c\,(t=0)$ the $\mathcal{V}_j$ should be constants independent of the system size L. In Fig. 3 we present this set of lines. From the linear fits to these points we estimate that $1/\nu=1.4391(78)$, which yields $\nu=0.6949(38)$. (The error in the final value for $1/\nu$ was determined from the errors in the individual estimates whose mean value is our final estimate.) With the critical exponent ν accurately determined we can use Eq. (22) to determine K_c as the extrapolation to $L\to\infty$ ($L^{-1/\nu}=0$) of the linear fits given by the locations of the maxima of the functions defined by Eqs. (17)–(21). In Fig. 4 we show this set of linear fits that converge to K_c at $L^{-1/\nu}=0$. To estimate the errors in our results, the location of the maximum of each thermodynamic function was determined several times (the number of times in each case varying from function to function and according to the size of the lattice), and the statistical error bars for each function in Fig. 4 is given as $\pm 1\sigma$, where σ is the standard deviation of the mean. The final estimate for K_c was taken as the mean of the five values obtained from fits for each thermodynamic function and was $K_c=1.342\,02(12)$ or $T_c=0.745\,15(7)$. If we compare with the Heisenberg ferromagnet[21] [$T_c=1.442\,92(8)$] we see that the phase transition in the double-exchange ferromagnet takes place at a lower temperature.

Since ν and T_c are now estimated to a high precision, we can calculate the critical exponents β and γ. According to Eq. (4), the maximum of the finite-lattice susceptibility defined by Eq. (17) and the true susceptibility at T_c, given by the same equation with $\langle m\rangle=0$, are both asymptotically proportional to $L^{\gamma/\nu}$. In Fig. 5 we show the two situations that yield $\gamma=1.3791(57)$ and $\gamma=1.4028(22)$, respectively. Since these values agree to within error bars of $\pm 2\sigma$, we can take their mean to obtain $\gamma=1.3909(30)$. In the vinicity of the critical temperature the magnetization varies as $L^{-\beta/\nu}$. We can use Eq. (3) at the critical point to calculate the exponent β directly from the slope of the log-log graph and find $\beta=0.3535(30)$. Our results are in good agreement with the scaling relation, Eq. (7), yielding $d\nu=2.085(11)$ and $2\beta+\gamma=2.089(10)$. [Note that the scaling law $\gamma/\nu=2-\eta$ then predicts a very small, negative estimate for η although the scaling law $\eta=2-d\gamma/(2\beta+\gamma)$ gives a very small but positive value.]

IV. DISCUSSION AND CONCLUSIONS

It is interesting to compare the exponents ν, β, and γ as well as the value of the magnetization fourth-order cumulant at the transition temperature, U^*, obtained for the classical ferromagnet with double-exchange interaction with those calculated for the Ising and Heisenberg model. In Table I we

TABLE I. Estimates of ν, β, γ, and U^* compared to the results for the Heisenberg and Ising models and some experimental data.

	ν	β	γ	U^*	Ref.
Double-exchange	0.6949(38)	0.3535(30)	1.3909(30)	0.62062(38)	Our results
Heisenberg	0.7036(23)	0.3616(31)	1.3896(70)		21
Heisenberg	0.704(6)	0.362(4)	1.389(14)	0.6217(8)	24
Ising	0.6289	0.3258(44)	1.2470(39)		22
$La_{0.7}Sr_{0.3}MnO_3$		0.37(4)	1.22(3)		25
$La_{0.7}Sr_{0.3}MnO_3$		0.45(5)			26
$La_{0.7}Sr_{0.3}MnO_3$		0.295			27
$La_{0.8}Sr_{0.4}MnO_3$		0.50(2)			28

show these values along with some experimental results and three-dimensional. Ising and Heisenberg models values for comparison. One can see that all three exponents for the double-exchange system agree within error bars equal to $\pm 2\sigma$ with those of the classical Heisenberg system; furthermore, the values of U^* agree to within $\pm 1\sigma$ errors. We can then conclude with some confidence that these two models belong to the same universality class. At the present time the available experimental data are inconsistent with each other; however, if improved experiments are forthcoming and the resultant critical behavior shows deviations from Heisenberg behavior, it must be due to additional mechanisms other than double exchange.

ACKNOWLEDGMENTS

This research was supported in part by NSF Grant No. DMR-9727714. One of us, A.A.C., wishes to acknowledge support by CAPES–Brasilia, Brazil.

[1] C. Zener, Phys. Rev. **82**, 403 (1951).
[2] P.W. Anderson and H. Hasegawa, Phys. Rev. **100**, 675 (1955).
[3] A. Asamitsu, Y. Moritomo, R. Kumai, Y. Tomioka, and Y. Tokura, Phys. Rev. B **54**, 1716 (1996).
[4] A.J. Millis, P.B. Littlewood, and B.I. Shraiman, Phys. Rev. Lett. **74**, 5144 (1995).
[5] C.M. Varma, Phys. Rev. B **54**, 7328 (1996).
[6] N. Furukawa, J. Phys. Soc. Jpn. **63**, 3214 (1994).
[7] J.W. Lynn, R.W. Erwin, J.A. Borchers, Q. Huang, A. Santoro, J.L. Peng, and Z.Y. Li, Phys. Rev. Lett. **76**, 4046 (1996).
[8] A.M. Ferrenberg and R.H. Swendsen, Phys. Rev. Lett. **61**, 2635 (1988).
[9] A.M. Ferrenberg and R.H. Swendsen, Phys. Rev. Lett. **63**, 1195 (1989).
[10] M.E. Fisher, in *Critical Phenomena*, edited by M.S. Green (Academic, New York, 1971).
[11] M.E. Fisher and M.N. Barber, Phys. Rev. Lett. **28**, 1516 (1972).
[12] M.N. Barber, in *Phase Transitions and Critical Phenomena*, edited by C. Domb and J.L. Lebowitz (Academic, New York, 1974), Vol. 8.
[13] K. Binder, Z. Phys. B: Condens. Matter **43**, 119 (1981).
[14] K. Binder and D. Stauffer, in *Applications of the Monte Carlo Method in Statistical Physics*, edited by K. Binder (Springer, Berlin, 1987), p. 1.
[15] D.P. Landau, J. Magn. Magn. Mater. **31-34**, 1115 (1983).
[16] D.P. Landau and K. Binder, Phys. Rev. B **31**, 5946 (1985).
[17] D.P. Landau, R. Pandey, and K. Binder, Phys. Rev. B **39**, 12 302 (1989).
[18] P. Peczak and D.P. Landau, Phys. Rev. B **43**, 1048 (1991).
[19] V. Privman, P.C. Hohenberg, and A. Aharony, in *Phase Transitions and Critical Phenomena*, edited by C. Domb and J.L. Lebowitz (Academic, New York, 1991), Vol. 14, p. 1.
[20] N. Metropolis, A.W. Rosenbluth, M.N. Rosenbluth, A.H. Teller, and E. Teller, J. Chem. Phys. **21**, 1087 (1953).
[21] K. Chen, A.M. Ferrenberg, and D.P. Landau, Phys. Rev. B **48**, 3249 (1993).
[22] A.M. Ferrenberg and D.P. Landau, Phys. Rev. B **44**, 5081 (1991).
[23] P. Peczak, A.M. Ferrenberg, and D.P. Landau, Phys. Rev. B **43**, 6087 (1991).
[24] C. Holm and W. Janke, Phys. Rev. B **48**, 936 (1993).
[25] K. Ghosh, C.J. Lobb, and R.L. Greene, Phys. Rev. Lett. **81**, 4740 (1998).
[26] S.E. Lofland, V. Ray, P.H. Kim, S.M. Bhagat, M.A. Manheimer, and S.D. Tyagi, Phys. Rev. B **55**, 2749 (1997).
[27] M.C. Martin, G. Shirane, Y. Endoh, K. Hirota, Y. Moritomo, and Y. Tokura, Phys. Rev. B **53**, 14 285 (1996).
[28] Ch.V. Mohan, M. Seeger, H. Kronmüller, P. Murugaraj, and J. Maier, J. Magn. Magn. Mater. **183**, 348 (1998).